Available online at www.sciencedirect.com
SCIENCE DIRECT®
Journal of Power Sources 119–121 (2003) 16–23
JOURNAL OF POWER SOURCES
www.elsevier.com/locate/jpowsour

Preparation and characterization of carbon nanotubes for energy storage

G.X. Wang*, Jung-ho Ahn, Jane Yao, Matthew Lindsay, H.K. Liu, S.X. Dou

Battery Technology Research Program, Institute for Superconducting and Electronic Materials, University of Wollongong, Wollongong, NSW 2522, Australia

Abstract

Multiwall carbon nanotubes (MWNTs) were synthesized using chemical evaporation deposition (CVD). The morphology and microstructure of MWNTs were observed via HRTEM. The multiwall carbon nanotubes are entangled to bundles with a diameter of several tens of nanometers. Electrochemical properties of MWNTs were examined via a variety of electrochemical testing techniques. The MWNTs electrode demonstrated a reversible lithium storage capacity of 340 mAh/g with good cyclability at moderate current density. The kinetic properties of lithium insertion in MWNTs electrodes were characterized via ac impedance measurements. It was found that the lithium diffusion coefficient D_{Li} decreases with an increase of Li-ion concentration in MWNTs electrodes.

Keywords: Multiwall carbon nanotubes; Chemical vapor deposition; Li-ion battery; ac impedance

1. Introduction

Carbon nanotubes (CNTs) were discovered by Iijima [1], who produced helical microtubules of graphitic carbon using an arc-discharge evaporation method. Since then, tremendous interest and effort have been devoted to the production, characterization and application of carbon nanotubes. In general, carbon nanotubes can be classified as two categories, e.g. multiwall carbon nanotubes (MWNTs) and single wall carbon nanotubes (SWNTs). MWNTs consist of graphitic sheets rolled into closed concentric cylinders, in which the concentric tube are in a distance of ~3.4 Å. The external diameters of MWNTs can range from a few nanometers to tens of nanometers [2]. The length of MWNTs can be of several micrometers. SWNTs are defined by a cylindrical graphene sheet with a diameter of about 0.7–10.0 nm. Therefore, SWNTs have a large ratio of length to diameter, which can be as large as 10^4 to 10^5. These SWNTs nanotubes can be considered as one-dimensional nanostructures [3].

Carbon nanotubes can be produced using various techniques such as electric arc-discharge [4,5], laser vaporization [6,7] and chemical vapor deposition [8–10]. Since carbon nanotubes have unique structural, mechanical, electronic and electrical properties, they are an attractive system standing for wide range applications such as nanoscale electronic devices [11], chemical filter, energy storage [12] and electron field emission sources.

Since various carbonaceous materials can reversibly react with lithium in Li-ion cells, carbon nanotubes have been speculated to the applications as lithium insertion hosts for Li-ion batteries [13–15]. It has been reported that carbon nanotubes demonstrated reversible lithium storage capacity in the range of 80–600 mAh/g. The electrochemical performance of carbon nanotubes strongly depends on their structure, morphology and disorder. In this investigation, multiwall carbon nanotubes were produced using chemical vapor deposition (CVD). The electrochemical properties of these MWNTs were systematically examined.

2. Experimental

The MWNTs were prepared by catalytic CVD using a nanosized cobalt as catalyst. During the production of MWNTs, about 100 mg catalyst was placed in a quartz tube mounted in a tube furnace. The furnace was initially evacuated and then purged with argon gas. The furnace was then heated to 800–1000 °C with argon flow. The argon was then

* Corresponding author. Fax: +61-2-42215731.
E-mail address: gwang@uow.edu.au (G.X. Wang).

0378-7753/03/$ – see front matter © 2003 Elsevier Science B.V. All rights reserved.
doi:10.1016/S0378-7753(03)00117-4

replaced by acetylene at a flow rate of 100–500 ml/min for 20–60 min. The synthesized CNTs were then annealed at 900 °C for 1 h before being allowed to cool down.

The microstructure and morphology of MWNTs were observed using JEOL EM 2010 HRTEM microscope. X-ray diffraction (XRD) measurements were carried out on a Mo3xHF22 diffractometer (MacScience Co. Ltd., Japan). The Teflon testing cells were fabricated to test the electrochemical properties of carbon nanotubes as anodes in Li-ion cells. The carbon nanotube electrodes were made by dispersing 95 wt.% carbon nanotube powders and 5 wt.% polyvinylidene fluoride (PVDF) binder in dimethyl phthalate solvent to form a slurry, which was then pasted onto a nickel foam. The electrodes were dried at 120 °C in a vacuum oven for 24 h. The two-electrode testing cells were assembled for charge/discharge testing. For cyclic voltammetry and ac impedance measurements, three-electrode test cells were prepared, in which the counter electrode and reference electrode were lithium foil. The cells were assembled in an argon filled glove-box (Mbraun, Unilab, USA). The electrolyte was 1 M $LiPF_6$ in a mixture of ethylene carbonate (EC) and dimethyl carbonate (DMC) (1:1 by volume, provided by MERCK KgaA, Germany). The cells were galvanostatically charged and discharged at different current densities, and showed voltage behavior over the voltage range 0.01–3.0 V versus Li/Li^+. Cyclic voltammetry (CV), was performed to determine the characteristics of lithium reaction with carbon nanotubes electrodes. The CV measurements were carried out on a potentiostat (Model M362, EG&G Princeton Applied Research, USA) at a scanning rate of 0.1 mV/S. The ac impedance measurement was performed on the as-prepared carbon nanotubes electrodes at different potentials. Before ac impedance measurements, the cell was pre-cycled galvanostatically between 3.0 and 0.05 V for five cycles to establish and stabilize the solid electrolyte interface (SEI) between the electrolyte and carbon nanotube electrode. The cell was potentiostatically conditioned to a certain potential and equilibrated for 3 h. After then, the ac impedance spectroscopy was obtained by applying a sine wave of 5 mV amplitude over the frequency range of 100 kHz to 10 mHz.

3. Results and discussion

3.1. Microstructural characterization

The XRD pattern of as prepared carbon nanotubes is shown in Fig. 1. The (0 0 2) and (1 0 1) diffraction lines are the only distinguishable diffraction peaks. Both of these two diffraction peaks are broadened. The $d_{0\,0\,2}$ value derived from this XRD pattern is 3.44 Å, which is slightly higher than that of the perfect graphite ($d_{002} = 3.35$ Å). From XRD pattern, it can be concluded that the prepared carbon nanotubes are partially graphitized. The morphology and microstructure of carbon nanotubes were characterized by HRTEM. Fig. 2 shows the morphologies of the as-prepared multiwall carbon nanotubes. As shown in Fig. 2(a), most of carbon nanotubes are entangled together to form bundles or ropes. The diameter of the carbon nanotubes is in the range of 20–50 nm. There is a small amount of amorphous carbon particles presented in this sample. However, the yield of carbon nanotubes is more than 95%. By carefully observing the tips of carbon nanotubes, it can be found that the tips of each nanotubes are closed, typically with a curly shape. Fig. 2(b) shows the view of a single carbon nanotubes, which has a typical bamboo structure. The bamboo shape indicates that the carbon nanotubes have grown according to a certain kinetic mechanism. It clearly demonstrated the central hollow cylinder structure. The diameter of a single carbon nanotube is around 20–50 nm.

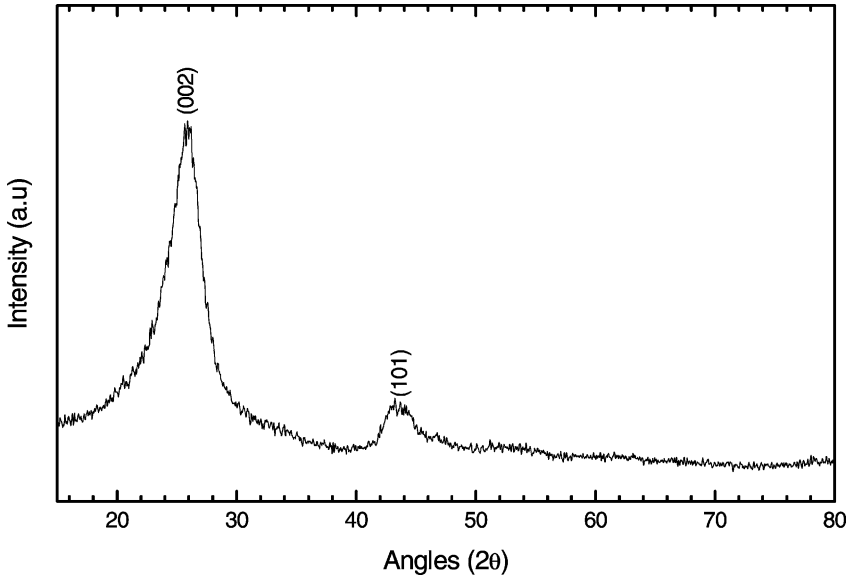

Fig. 1. X-ray diffraction patterns of multiwall carbon nanotubes.

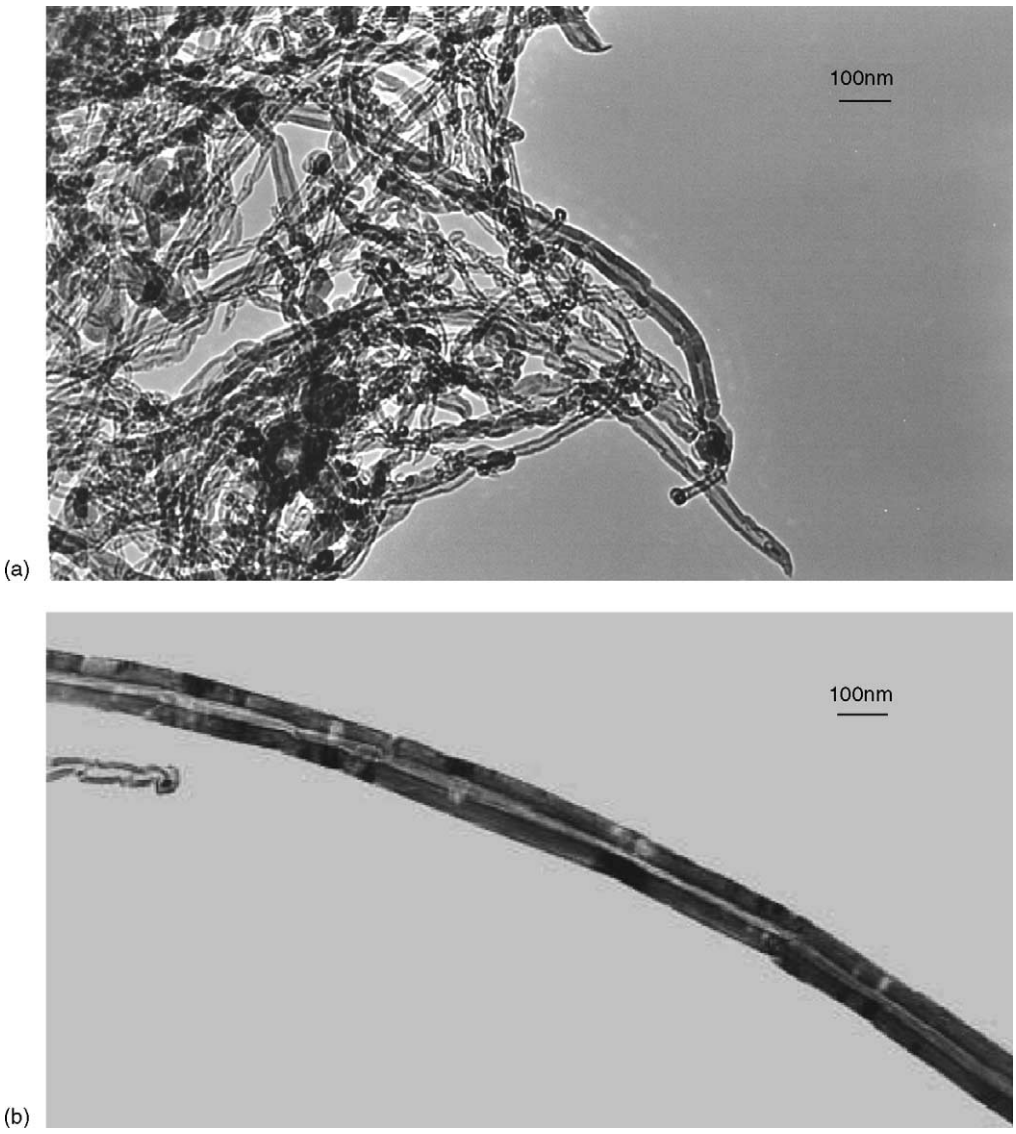

Fig. 2. HRTEM images of MWNTs.

3.2. Electrochemical testing of carbon nanotubes electrodes

Cyclic voltammetry of carbon nanotubes electrodes was measured, in which lithium foils were used as both working electrode and reference electrode. Fig. 3 shows the CV curves of the MWNTs electrode. The CV measurement of the MWNTs electrode demonstrated that lithium could reversibly intercalate and de-intercalate into carbon nanotubes electrode. The lithium insertion potential is quite low, which is very much close to 0 V versus Li^+/Li reference electrode, whereas, the potential for lithium de-intercalation is in the range of 0.2–0.4 V. The intensity of redox peaks of MWNTs decrease with scanning cycle, indicating that the reversible lithium insertion capacity gradually decreases.

The cyclability of the prepared carbon nanotubes electrodes was further tested at various different current densities. Fig. 4 shows the first discharge and subsequent discharge curves of carbon nanotubes electrode at a current density of 25 mA/g. The first discharge curve shows a plateau at about 0.8 V. This discharge plateau probably relates to the formation of a SEI film (solid electrolyte interface) on the surface of the carbon nanotubes, which is associated with electrolyte decomposition and the formation of lithium organic compounds. The discharge plateau at 0.8 V occupies a capacity of about 350 mAh/g and is not reversible. In the subsequent cycles, this discharge plateau disappeared. A reversible capacity of 320 mAh/g was obtained in the subsequent cycle, which is very similar to some graphite anode materials. The lithium trapped in these regions may be not reversible. To test the rate capacity of carbon nanotube electrodes, the cells were cycled at different current densities. Fig. 5 shows the lithium insertion capacity versus cycle number at different current densities. After the first cycle, the reversible capacity starts to stabilize at a certain level, which depends on the current density. It was found that lithium insertion capacity for carbon

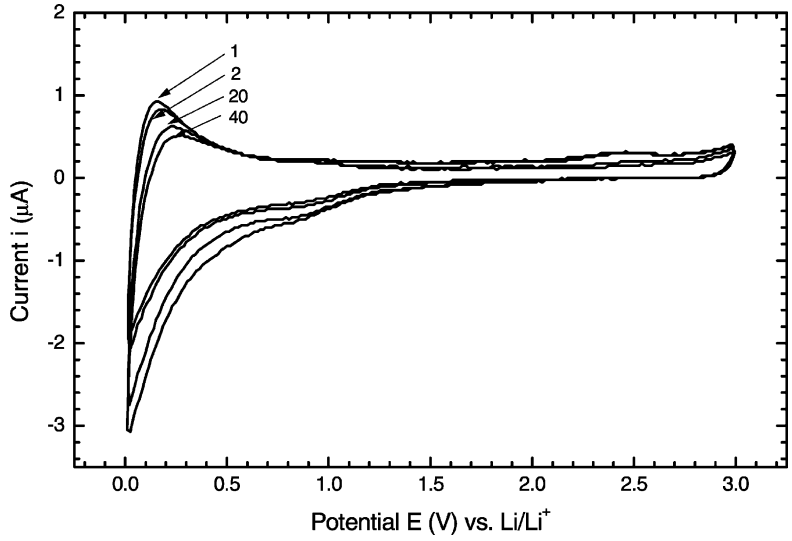

Fig. 3. Cyclic voltammogram of MWNTs electrode in Li-ion cell.

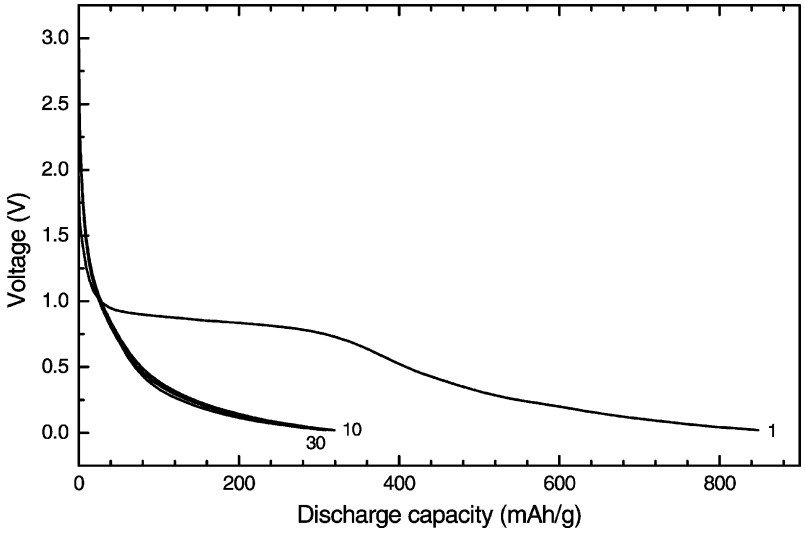

Fig. 4. The discharge curve of MWNTs electrode. Current density: 25 mA/g.

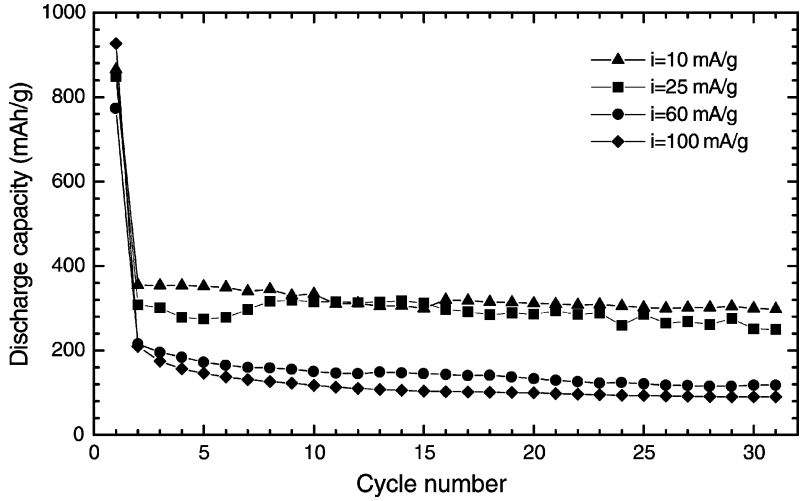

Fig. 5. The capacity vs. cycle number for MWNTs electrode at different current densities.

nanotubes electrodes is sensitive to current density. At a relatively low current density of 10 mA/g, a reversible lithium insertion capacity of 340 mAh/g was obtained up to 30 cycles. When the carbon nanotubes electrodes were charged and discharged at high current density, the reversible capacity was much lower than that at low current density. According to the "Russian doll" model, MWNTs consist of graphitic sheets rolled into closed concentric cylinders [1]. The concentric tubes are separated by van der Waals gaps of ~3.4 Å, a typical interlayer spacing in turbo statically disorder graphite. Assuming lithium ions can only combine every second hexagons on the external surface of rolled graphene sheet, the limiting stoichiometry would be less than LiC_6 in principle. So, the maximum lithium insertion should be less than the theoretical capacity of graphite 372 mAh/g, assuming the formation LiC_6 intercalation compound. The reversible lithium insertion capacity achieved for MWNTs at low current density was about 340–350 mAh/g, which matches the above assumption.

3.3. Electrochemical ac impedance spectroscopy

The ac impedance spectra of carbon nanotube electrodes were measured both during the lithium insertion and lithium

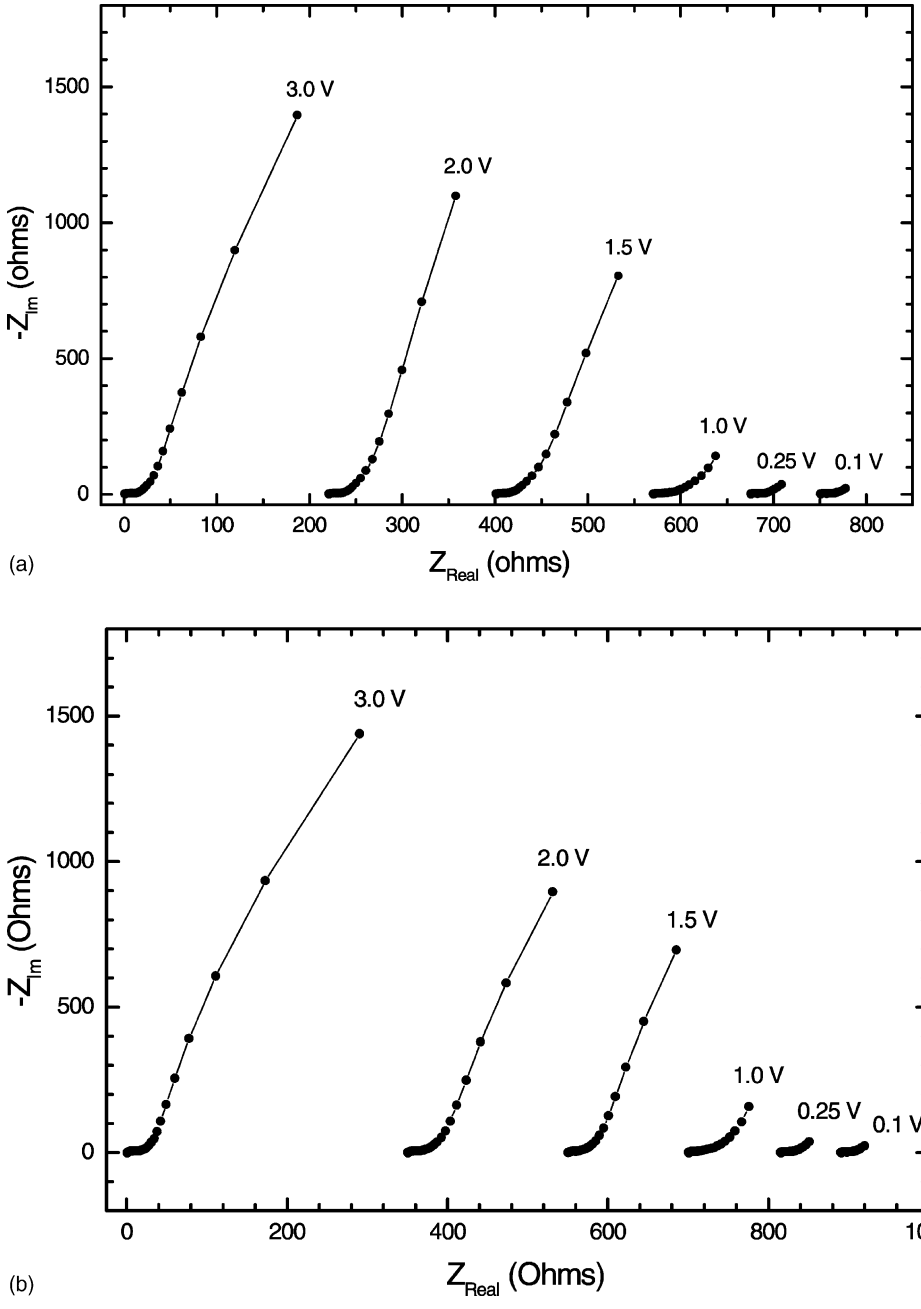

Fig. 6. The ac impedance diagrams of MWNTs electrodes at different potential (a) during lithiation process (b) during de-lithiation process. The frequency range: 100 kHz–0.01 Hz.

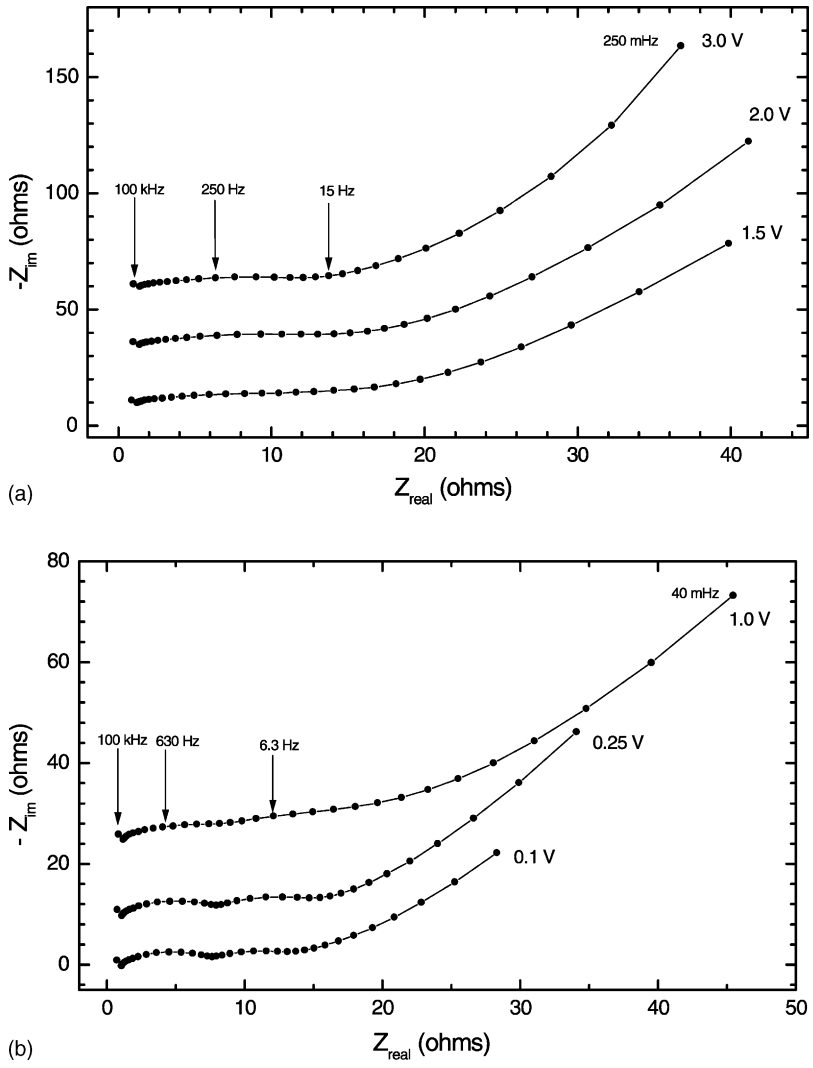

Fig. 7. The high frequency portion of ac impedance spectra of MWNTs electrode during lithiation process. The frequency range: 100 kHz–0.01 Hz.

de-intercalation processes. The Nyquist complex plane impedance plots are presented in Figs. 6 and 7. The ac impedance spectra measured in the lithiation process and in the de-lithiation process are surprisingly similar. This fact clearly demonstrates that carbon nanotube electrodes are stabilized after several charge/discharge cycles. At potentials of 3.0, 2.0 and 1.5 V, the MWNTs electrode exhibited the behavior of a blocking electrode in its impedance spectrum, which shows a linear line approaching an angle of 90° to Z_{im} axis. This indicates the amount of lithium intercalation is negligible in the potential range of 3.0–1.5 V [15]. As shown in Fig. 3, it can also be seen that lithium insertion starts from 1.5 V. The high frequency parts of the impedance spectrum are emphasized in Fig. 8. At a potential above 1.5 V, only one semicircle is observed in the high frequency regime (see Fig. 8(a)). However, in the potential regime below 1.5 V, two semicircles were observed in the high and medium frequency regime (see Fig 8(b)). An inclined line appeared in the low frequency region. Since the electrode has been pre-cycled for five cycles prior to the ac impedance measurement, a surface film has been established on the electrode/electrolyte interface. The high frequency semicircle is attributed to the impedance of Li ions migration through the surface films and surface films capacitance. The semicircle in the middle frequency region can be assigned to the charge-transfer impedance on the MWNTs electrode/electrolyte interface. The charge-transfer resistance consists of two parts. One is the electronic resistance and the other is ionic in nature due to the resistance of ion transfer across the electrolyte/electrode interface. The tail at approximate 45° angle to the real axis is attributed to the lithium diffusion within the carbon nanotube electrode.

The ac impedance spectra for the MWNTs electrode can be modeled by a modified Randles equivalent circuit presented in Fig. 8 [16,17]. R_e is the electrolyte resistance, C_f and R_f are the capacitance and resistance of surface film formed on the electrode, C_{dl} and R_{ct} are the double layer capacitance and charge-transfer resistance, and Z_w is the Warburg impedance related to the diffusion of lithium ions

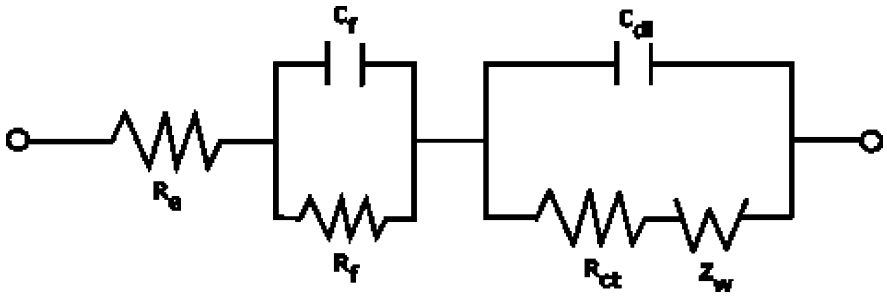

Fig. 8. Randles equivalent circuit model for MWNTs/electrolyte interface.

into the bulk of the MWNTs electrode. The exchange current density i_0 can be deduced from the equation of $i_0 = RT/nFR_{ct}$ [18]. The kinetic parameters are shown in Table 1. The magnitude of the variation of R_{ct} and i_0 is very small, indicating the stable nature of MWNTs, and also that the kinetics of the charge-transfer process are not affected during lithium insertion process. When the potential drops to 1.0 V, the high frequency regime shows two semicircles. This indicates that a surface film starts to build-up on the surface of the electrode. When the potential reaches 0.25 and 0.1 V, two well distinguishable semicircles are presented in the impedance spectrum (see Fig. 7(b)). It was found that the double layer capacitance C_{dl} changes significantly when the electrode potential drops to 0.25 V. This fact suggests the formation of the surface film greatly influences the double layer capacitance. The low frequency portion of the EIS spectra can be further divided into two regimes: a 45° line and a quasi-vertical line. The 45° line is thought to be due to lithium diffusion behavior, and the near-vertical tail is considered as an indication of finite length diffusion. At very low frequency, the MWNTs electrode can be treated as a capacitor C_L and a resistor R_L in series, sometimes referred to as limiting resistance and limiting capacitance respectively. The C_L value can be calculated using the formula $C_L = 1/\omega Z$ and the lowest frequency data. The lithium diffusion coefficients in MWNTs host can be deduced from the formula $D_{Li} = L^2/(3R_L C_L)$ where L is the maximum diffusion length [19,20]. Assuming lithium diffusion parallel to the carbon naotube bundle, in that case, the maximum diffusion pathway L is about 1 μm. The value of D_{Li} decreases with a decrease of the electrode potential. Since the Li concentration increases with decreasing electrode potential, therefore, it can be concluded that the lithium diffusion coefficient is affected by the Li concentration in the carbon nanotube host.

Table 1
Kinetic parameters of carbon nanotube electrode

Potential of MWNTs electrode (V)	R_{ct} (Ω/cm^2)	i_0 (A/cm^2)	C_{dl} (μF)	D_{Li}(cm^2/s)
3.0	19.66	1.3×10^{-4}	5.11	1.48×10^{-8}
2.0	22.86	1.12×10^{-4}	6.96	1.0×10^{-8}
1.5	19.85	1.29×10^{-4}	8.02	8.48×10^{-9}
1.0	15.88	1.62×10^{-4}	6.33	1.8×10^{-9}
1.25	16.33	1.57×10^{-4}	452	4.6×10^{-10}
0.1	15.97	1.6×10^{-4}	761	2.9×10^{-10}

4. Conclusion

Multiwall carbon nanotubes were successfully prepared by CVD method. The as-prepared MWNTs have a typical diameter about several tens of nanometers and entangled to bundles. The electrochemical testing shows MWNTs electrode can deliver a reversible capacity of 340 mAh/g in Li-ion cells, which is similar to some graphite electrode. Further improvement of the reversible lithium storage capacity is possible by reducing the structural defects of the carbon nanotubes. The kinetics of Li-ion insertion in MWNTs electrode were characterized by ac impedance measurement. The exchange current density i_0 is almost invariant with the variation of the electrode potential. But the lithium diffusion coefficient (D_{Li}) decreases significantly as the increase of Li concentration in MWNTs electrode.

Acknowledgements

The Financial support from Australia Research Council (ARC) is greatly acknowledged.

References

[1] S. Iijima, Nature 354 (1991) 56–58.
[2] S. Claye, E. Fischer, B. Huffman, G. Rinzler, E. Smalley, J. Electrochem. Soc. 147 (2000) 2845–2852.
[3] R. Saito, G. Dresselhaus, M.S. Dresselhaus, Physical Properties of Carbon Nanotubes, Imperial College Press, London, 1998, p. 35.
[4] T.W. Ebbesen, P.M. Ajayan, Nature 358 (1992) 220–222.
[5] S. Seraphin, D. Zhou, J. Jiao, J.C. Withers, R. Loufty, Carbon 31 (1993) 685.
[6] T. Guo, P. Nikolaev, A. Thess, D.T. Colbert, R.E. Smalley, Chem. Phys. Lett. 243 (1995) 49.
[7] M. Yudasaka, T. Komatsu, T. Ichihashi, S. Iijima, Chem. Phys. Lett. 278 (1997) 102.
[8] I. Willems, Z. Konya, J.-F. Colomer, G. Van Tendeloo, N. Nagaraju, A. Fonsea, J.B. Nagy, Chem. Phys. Lett. 317 (2000) 71.

[9] B.C. Satishkumar, A. Govindaraj, R. Sen, C.N.R. Rao, Chem. Phys. Lett. 293 (1998) 47.
[10] J. Kong, H. Soh, A.M. Cassel, C.F. Quate, H. Dai, Nature 395 (1998) 878.
[11] L. McEuen, Nature 393 (1998) 15.
[12] G.-L. Che, B.B. Lakshmi, E.R. Fisher, C.R. Martin, Nature 393 (1998) 346.
[13] E. Frackowiak, S. Gautier, H. Gaucher, S. Bonnamy, F. Beguin, Carbon 37 (1999) 61.
[14] G.T. Wu, C.S. Wang, X.B. Zhang, H.S. Yang, Z.F. Qi, P.M. He, W.Z. Li, J. Electrochem. Soc. 146 (1999) 1696.
[15] A. Funabiki, M. Inaba, Z. Ogumi, J. Power Sources 68 (1997) 227–231.
[16] P. Liu, H. Wu, J. Power Sources 56 (1995) 81–85.
[17] A.S. Claye, J.E. Fischer, C.B. Huffman, A.G. Rinzler, R.E. Smalley, J. Electrochem. Soc. 147 (2000) 2845–2852.
[18] N. Takami, A. Satoh, M. Hara, T. Ohsaki, J. Electrochem. Soc. 142 (1995) 371–378.
[19] C. Ho, I.D. Raistrick, R.A. Huggins, J. Electrochem. Soc. 127 (1980) 343.
[20] B. Garcia, J. Farcy, J.P. Pereira-Ramamos, N. Baffier, J. Electrochem. Soc. 144 (1997) 1179.